GASEOUS BINARY COUNTERDIFFUSION IN ACTIVATED CARBON

by

HOWARD SHELDON DENENHOLZ

Bachelor of Science

Illinois Institute of Technology

Chicago, Illinois

1965

Submitted to the faculty of the Graduate College
of the Oklahoma State University
in partial fulfillment of the requirements
for the degree of
MASTER OF SCIENCE
May, 1967

GASEOUS BINARY COUNTERDIFFUSION IN ACTIVATED CARBON

Thesis Approved:

_____
Thesis Adviser

_____

_____
Dean of the Graduate College

658672

PREFACE

The purpose of this work was to study gaseous binary counterdiffu-
sion in activated carbon in the transition regime. A gas diffusion
apparatus was built and used in this study. The experimental results
were analyzed according to two theoretical models: 1) Wakao-Smith model
from kinetic theory of gases; and 2) Rothfeld model from Fick's first
law of diffusion. Reasonable agreement was obtained with these models,
but further work along lines suggested should be pursued to better de-
termine the parameters which are needed for the calculations.

selecting and obtaining needed materials; and to Joan Neal for typing

the manuscript.

TABLE OF CONTENTS

LIST OF TABLES

LIST OF FIGURES

CHAPTER I

THEORY

Introduction

As adsorption processes are widely used in the chemical industry,
it becomes important that engineers have the means of predicting their
behavior. Reliable means of prediction are vital for the design and
operation of such processes.

Adsorption processes are characterized by the mass transfer of the
adsorbate from the surrounding fluid into the interior of the adsorbent.
At the conditions of industrial operations of fixed beds of activated
carbon, the major part of the overall resistance to the mass transfer
is contributed by diffusion within the carbon pellets. There is con-
siderable motivation to be able to predict the diffusion rate. This
study is undertaken with the objective of (1) providing some basic
diffusion rate data in activated carbon, and (2) extending the useful-
ness of the data by comparing them with theoretical calculations to
permit meaningful conclusions to be drawn concerning their applicability
to activated carbons.

In this experiment, the steady-state method of measuring diffusion
rates was used. The transient method of measuring diffusion rates was
used by some authors (8) in the past. It was decided not to use the
latter because of the complications due to the accompanying heat trans-
fer problems and the presence of net flow and a pressure gradient within

1

the pellet.

Several regimes of diffusion in porous materials can be discerned.
The criteria for regime designation is the ratio of the mean free path to
the dimension of the pores in the absorbent. When the mean free path is
much smaller, the gas is in bulk diffusion. If the reverse is true, the
gas is in Knudsen diffusion. For the case where the dimensions are simi-
lar, the gas is in the transition or slip regime. Knudsen diffusion is
the limiting case where the molecules act independently of each other
while bulk diffusion is the other limiting case where the gas acts as a
continuum.

The Knudsen and bulk diffusion regimes have been well described for
capillaries (12). Recently research interest has turned to the slip re-
gime of diffusion in porous materials. Many theories have been presented,
but few fit experimental data with reliability (10). Two of the more
promising for binary counterdiffusion are those developed by Rothfeld (9)
and Wakao-Smith (13). For comparison to an elementary theory, the straight
parallel capillary tube bundle model was included in the investigation.

Straight Tube Model

Three basic theories are pertinent to the discussion of diffusion
in porous material. These are: (1) the straight-parallel capillary
tube bundle model; (2) the Wakao and Smith model; and (3) the Rothfeld
model. The basic differential equation can be derived from either funda-
mental kinetic theory of gases or from Fick's first law of diffusion.

Many textbooks on kinetic theory of gases contain the development
of the basic differential equation for isothermal, isobaric steady-state
counterdiffusion. Based on considerations of rate of momentum transfer,

Present (7) shows

$$-dp_A (\pi r^2) = \frac{u_A n_A m_A \bar{v} (2\pi r) dL}{4} + n_A n_B (u_A - u_B) \frac{kT \pi r^2 dL}{n_T \mathcal{D}_{AB}} \tag{1}$$

where the symbols are explained in the Nomenclature section. Equation (1) assumes that elastic collisions occur everywhere in the circular duct. The first term accounts for momentum transfer in collisions with the wall while the second term accounts for momentum transferred in collisions of unlike molecules. It is assumed both contribute importantly to the overall momentum transfer (11).

Using the following definitions

$$\bar{D}_{KA} = \frac{2}{3} \bar{v}_A \bar{r}$$

$$\bar{v}_A = (8RT/\pi M_A)^{1/2} \tag{2}$$

$$\alpha = 1 - |N_B/N_A|$$

$$dp_A = P dy_A$$

Equation (1) becomes

$$-P dy_A / (N_A RT dL) = 8/(3\pi \bar{D}_{KA}) + (1 - \alpha y_A)/\mathcal{D}_{AB} \tag{3}$$

In the literature, the factor $8/(3\pi)$ is taken as one. Hence Equation (3) becomes

$$-P dy_A / (N_A RT dL) = 1/\bar{D}_{KA} + (1 - \alpha y_A)/\mathcal{D}_{AB} \tag{4}$$

Using the following boundary conditions

$$y_A = y_{AO} \text{ at } L = 0$$

$$y_A = y_{AL} \text{ at } L = L \tag{5}$$

Equation (4) is integrated to yield

$$N_A = \frac{P \mathcal{D}_{AB}}{RTL\alpha} \ln \frac{1 - \alpha y_{AL} + \mathcal{D}_{AB}/\overline{D}_{KA}}{1 - \alpha y_{AO} + \mathcal{D}_{AB}/\overline{D}_{KA}} \tag{6}$$

where N_A is the flux per unit flow area. For a bundle of such

capillaries, Equation (6) can be written as

$$N_A = \frac{eP \mathcal{D}_{AB}}{RTL\alpha} \ln \frac{1 - \alpha y_{AL} + \mathcal{D}_{AB}/\overline{D}_{KA}}{1 - \alpha y_{AO} + \mathcal{D}_{AB}/\overline{D}_{KA}} \tag{7}$$

since the flux per unit area available for flow should remain the same.

The porosity (e) is used to convert the area from area available for

flow to total area of the bundle.

Wakao and Smith Model

In 1962, Wakao and Smith (13) presented their theory of diffusion

in bidispersed porous materials with constant pressure throughout the

material. Their model proposes that the diffusion in porous material

is a combination of diffusion through macro- and micropores, the rela-

tionship between the two systems depends on the relationship of their

respective porosities. Figure 1 illustrates the system proposed by Wakao

and Smith for diffusion. The shaded areas represent the particles con-

taining the micropores and the open areas represent the macropores. They

also assume the area fractions equal the volume fractions. Thus the prob-

ability that a given point (on a plane orthogonal to the direction of

diffusion) will be in a void is e. Where e is the volume void fraction.

They then cut the sample at the plane and rejoin the two surfaces. The

probability of a point being in a void on both sides of the plane will be

that of two successive events or e^2. This probability also represents
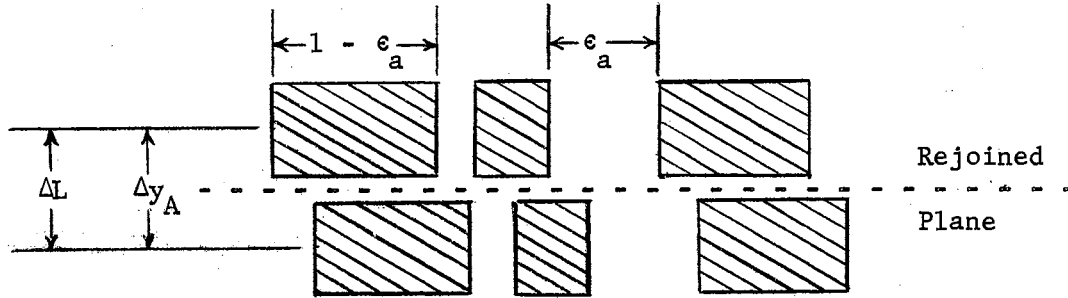
Figure 1. Wakao and Smith Model of Porous Material

the void area.

Diffusion through the plane is divided into three parallel mechanisms:

1.) Through the macropores of area ε_a^2.

2.) Through the micropores of area $\varepsilon_i^2 / (1 - \varepsilon_a)^2$ contained in particles having an area of $(1 - \varepsilon_a)^2$.

3.) Through the macropores and micropores in series for which the area is $1 - \varepsilon_a^2 - (1 - \varepsilon_a)^2$ or $2\varepsilon_a (1 - \varepsilon_a)$.

Then using Equation (4), they combine the three mechanisms as follows:

$$N_A \frac{RT}{P} = -\varepsilon_a^2 D_a \frac{\Delta y_A}{\Delta L} - (1 - \varepsilon_a)^2 D_i \frac{\Delta y_A}{\Delta L} - \frac{2\varepsilon_a (1 - \varepsilon_a)}{(1/D_a + 1/D_i)} \frac{2 \Delta y_A}{\Delta L} \qquad (8)$$

Here the unit cell of length ΔL is repeated to make up the pellet. ΔL is from the center of one particle to that of its neighbor. Δy_A is the concentration change across the element. The diffusivities D_i and D_a are for the micro and macro regions respectively and are given by

$$D_a = 1 / ((1 - \alpha y_A) / \mathcal{D}_{AB} + 1 / \bar{D}_{KA}) \qquad (9)$$

$$D_i = (\epsilon_i^2 / (1 - \epsilon_a)^2) / ((1 - \alpha y_A)/\mathcal{D}_{AB} + 1/\bar{D}_{KA}) \tag{10}$$

Summing Equation (8) over the entire pellet yields

$$N_A \frac{RTL\alpha}{P\mathcal{D}_{AB}} = \epsilon_a^2 \ln \frac{1 - \alpha y_{AL} + \mathcal{D}_{AB} / \bar{D}_{KAa}}{1 - \alpha y_{AO} + \mathcal{D}_{AB} / \bar{D}_{KAa}} +$$

$$+ \epsilon_i^2 \ln \frac{1 - \alpha y_{AL} + \mathcal{D}_{AB}/\bar{D}_{KAi}}{1 - \alpha y_{AO} + \mathcal{D}_{AB}/\bar{D}_{KAi}} +$$

$$+ \frac{4\epsilon_a (1 - \epsilon_a)}{1 + ((1-\epsilon_a)/\epsilon_a)^2} \ln \frac{1-\alpha y_{AL} + \dfrac{\mathcal{D}_{AB}}{\bar{D}_{KAi}} \dfrac{((1-\epsilon_a)/\epsilon_a)^2 + \bar{D}_{KAi}/\bar{D}_{KAa}}{1 + (1 - \epsilon_a)^2/\epsilon_a^2}}{1 - \alpha y_{AO} + \dfrac{\mathcal{D}_{AB}}{\bar{D}_{kAi}} \dfrac{((1-\epsilon_a)/\epsilon_a)^2 + \bar{D}_{KAi}/\bar{D}_{KAa}}{1 + (1 - \epsilon_a)^2/\epsilon_a^2}}$$

$$\tag{11}$$

Rothfeld Theory

Rothfeld (8) derives the straight tube model for porous material using Fick's first law of diffusion definitions as follows:

1.) Effective diffusion coefficient

$$\vec{J}_A^* = - c \, D_{AB} \nabla y_A \tag{12}$$

2.) Diffusion tortuousity for bulk diffusion by

$$(\vec{J}_A^*)_{bulk\ diffusion} = -\epsilon \, \mathcal{D}_{AB} c\nabla y_A /q \tag{13}$$

3.) Knudsen diffusion coefficient

$$(\vec{J}_A^*)_{Knudsen\ diffusion} = -\mathcal{D}_{AB}^K c\nabla y_A \tag{14}$$

where $\mathcal{D}_{AB}^{K} = \mathcal{D}_{BA}^{K} = \overline{D}_{KA} (1 - y_A (1 - R_{AB}))$ $\qquad$ (15)

Using the Stephan-Maxwell momentum balance method, Rothfeld (8) derives

$$D_{AB}^{-1} = q (\epsilon \mathcal{D}_{AB})^{-1} + (\mathcal{D}_{AB}^{K})^{-1} \qquad (16)$$

Equation (16) is very similar to Bosanquet's formula for the effective diffusion coefficient for self-diffusion. Combining Equation (15) and (16) yields

$$D_{AB} = (\epsilon \mathcal{D}_{AB}/q) (1 - y_A (1 - R_{AB}))/((\epsilon \mathcal{D}_{AB}/q \overline{D}_{KA}) + (1 - y_A (1 - R_{AB})) \qquad (17)$$

The familiar relationship between $\vec{N}_A$ and $\vec{J}_A^*$

$$\vec{N}_A = \vec{J}_A^* + y_A (\vec{N}_A + \vec{N}_B) \qquad (18)$$

is combined with Equations (17) and (12) to yield

$$\vec{N}_A = -(\epsilon \mathcal{D}_{AB} c \nabla y_A/q)/((\epsilon \mathcal{D}_{AB}/q D_{KA}) + 1 - y_A (1 - R_{AB})) \qquad (19)$$

In a cylindrical pellet where only the parallel faces are exposed to the gases, Equation (19) can be rewritten as

$$N_A = \frac{-(\epsilon \mathcal{D}_{AB}/q) c}{(\epsilon \mathcal{D}_{AB}/q \overline{D}_{KA}) + 1 - \alpha y_A} \frac{dy_A}{dL} \qquad (20)$$

where $\alpha = 1 - R_{AB}$

Integration of Equation (20) using the boundary conditions in Equation (5) yields

$$N_A \left(\frac{Lq\alpha}{\epsilon c \mathcal{D}_{AB}}\right) = \ln \frac{(\epsilon \mathcal{D}_{AB}/q \overline{D}_{KA}) + 1 - \alpha y_{AL}}{(\epsilon \mathcal{D}_{AB}/q \overline{D}_{KA}) + 1 - \alpha y_{AO}} \qquad (21)$$

When $y_{AL} = 0$ and $y_{AO} = 1$, Equation (21) reduces to

$$N_A \frac{Lq\alpha}{\epsilon c \cancel{D}_{AB}} = \ln \frac{(\epsilon \cancel{D}_{AB}/q \, \bar{D}_{KA}) + 1}{(\epsilon \cancel{D}_{AB}/q \, \bar{D}_{KA}) + R_{AB}} \tag{22}$$

Then from intuition Rothfeld developed the following relationship which

fits Equation (22) within a few per cent

$$\frac{c \, \bar{D}_{KA}}{N_A L} = 1 + \frac{q \, \bar{D}_{KA} \, (R_{AB}-1)}{\epsilon \cancel{D}_{AB} \, \ln R_{AB}} \tag{23}$$

The first term gives the flux for the Knudsen diffusion limit while

the second term is the bulk diffusion limit (9). When all the data

falls in the Knudsen range, the slope is zero and for the bulk diffusion

regime the intercept is essentially zero (9).

Further Modifications

There are several variations of the basic diffusion equation in

the literature. These variations will also be investigated. First the

Knudsen diffusion coefficient derived by Deryaguin (6) will be substi-

tuted for the usual Knudsen coefficient. The difference between the two

is that the present coefficient assumes elastic collisions with the wall

while Deryaguin's coefficient assumes inelastic collisions. Deryaguin's

coefficient is given as

$$\bar{D}_{DKA} = \frac{6}{13} \, \bar{r} \, (8 \, RT/\pi M_A)^{\frac{1}{2}} \tag{24}$$

Rothfeld (9) suggested using a Wheeler type coefficient in place of

the Bosanquet type effective diffusion coefficient. A Wheeler effective

diffusion coefficient is

$$D_{AB} = \mathcal{D}_{AB} \left(1 - \exp\left(-\overline{D}_{KA}/\mathcal{D}_{AB}\right)\right) \tag{25}$$

while the Bosanquet effective diffusion coefficient is

$$D_{AB}^{-1} = D_{KA}^{-1} + \mathcal{D}_{AB}^{-1} \tag{26}$$

By replacing Equation (26) in Equation (4) with Equation (25), the following is obtained

$$N_A dL = \frac{(\mathcal{D}_{AB} \, P \, /RT) \, dy_A}{\left(1 \, / \, \left(1 - \exp\left(-\overline{D}_{KA}/\mathcal{D}_{AB}\right)\right) - \alpha y_A\right)} \tag{27}$$

Integrating Equation (27) using Equation (5), the following result is yielded for the straight tube model

$$N_A = \frac{P\mathcal{D}_{AB}}{RTL\alpha} \, \ln \frac{1/\left(1 - \exp\left(-\overline{D}_{KA}/\mathcal{D}_{AB}\right)\right) - \alpha y_{AL}}{1/\left(1 - \exp\left(-\overline{D}_{KA}/\mathcal{D}_{AB}\right)\right) - \alpha y_{AO}} \tag{28}$$

For a bundle of such tubes the flux would be given by multiplying the right side by the porosity. This equation could also be changed to be used for porous material by multiplying the bulk diffusion coefficients by the quantity (ε/q) as Rothfeld suggests. However, here it will be used as a straight tube model as a preliminary investigation.

CHAPTER II

EXPERIMENTAL

Equipment

The equipment used in this experiment is of simple construction
except for the gas chromatograph. Modular construction is used so that
each section can be sealed off from the others for cleaning, modification,
or between runs. The modules are the gas chromatograph, the diffusion
cell, and the flowmeter system as shown in Figure 2.

The heart of the gas chromatograph module is a Micro-Tek GC-2500R
gas chromatograph equipped with Micro-Tek's standard thermoconductivity
cell and the recommended Honeywell recording potentiometer. The two
chromatograph columns are packed with ten grams each of Porapak Type Q,
50-80 mesh, in 1/4-inch stainless steel tube columns. One column is
used as a reference and the other for separating the sample. Both
columns are packed because the samples are injected into either one.
The column into which the sample is injected depends on which side of
the diffusion cell is sampled.

Sampling of the diffusion cell is done with the aid of two Micro-Tek
linear gas sampling valves (catalog number 713107) which are connected
directly to the exit lines of the diffusion cell. These valves allow
samples to be taken and injected into the chromatograph without any
chance of contamination. The sample loops of the sampling valves were
decreased in size to prevent flooding of the chromatograph columns.

10

Sizing the sample loops was a trial and error procedure to find one
which did not cause column flooding.

To maintain a constant pressure in the sample loops a Manostat
Corporation Model 8 Cartesian Manostat and a Merriam mercury manometer
were used in conjunction with a Duo-Seal vacuum pump. A constant
pressure in the sampling loop is necessary to assure results consistent
with the calibration runs.

Heavy walled stainless steel capillary tubing is used for the flow-
meter. The tubes are 1/8-inch outside diameter and six feet long with
a nominal inside diameter of 1/2 millimeter. Pressure at the high
pressure end of the capillary is measured with a thirty inch U-tube
manometer made of seven millimeter glass tubing and filled with mercury.
The same type of glass tubing is used to make the thirty-six inch high
U-tube filled with technical grade triethylene glycol (TEG) which
measures the pressure drop across the capillary. TEG is used because of
its low density and extremely low vapor pressure. The flowmeters are
connected to the gas supply tank through a series of Nupro B2M valves
to reduce the pressure. Each valve is separated from its neighbor by a
minimum of six feet of copper tubing to allow recovery of ambient
temperature (the number of valves varies with tank outlet pressure).
To reduce the number of manometer blowouts during the adjustment
periods, three-way teflon stopcocks are used to connect the manometers
to the high pressure side of the capillaries. All tank regulators are
those recommended by the Matheson Company for the various tank heads
and pressures.

The diffusion cell as assembled is shown in Figure 2. The glass
parts of the cell were made in the Chemistry Department Glass Shop

following the design suggested by Rothfeld (8). The cell is divided into chambers by a copper ring in which the sample pellet is mounted. A pure gas impinges on each face of the sample pellet, and is removed around the circumference of the chamber. The diffusion fluxes through the carbon pellet are determined by measuring the flow rates of the incoming pure gases and the concentrations of the exiting gas streams. Absolute pressure in the cell is measured using a thirty inch glass U-tube filled with mercury. To assure no static pressure difference across the pellet an RGI Positive Closed End Manometer filled with TEG was connected to the chambers separated by the pellet. Used in this manner this manometer is accurate to ± 0.01 centimeters.

The carbon pellets were mounted in brass rings specifically made to fit the micrometer measured diameters of the pellets. The brass ring is then mounted in Tygon tubing which is then used to connect the two halves of the cell together. The cell is connected to the rest of the system with Swaglok unions. The unions are connected on one side to the glass diffusion cell by means of Teflon ferrules. The other sides are connected to Tygon tubing.

The use of short lengths of flexible tubing is necessary to prevent stress on the glass cell. The overall volume of the system is small enough to allow it to be flushed in about thirty seconds. (The gases enter at the rate of one to three cubic centimeters per second.)

Two pieces of auxiliary equipment are worth mentioning. One is a vessel for reactivating the carbon pellets. It is made from a copper sampling bomb with one end sealed and the other end fitted with a connection to a vacuum pump. The other one is a precision cathetometer that is used to read all the manometers to ± 0.01 centimeter.
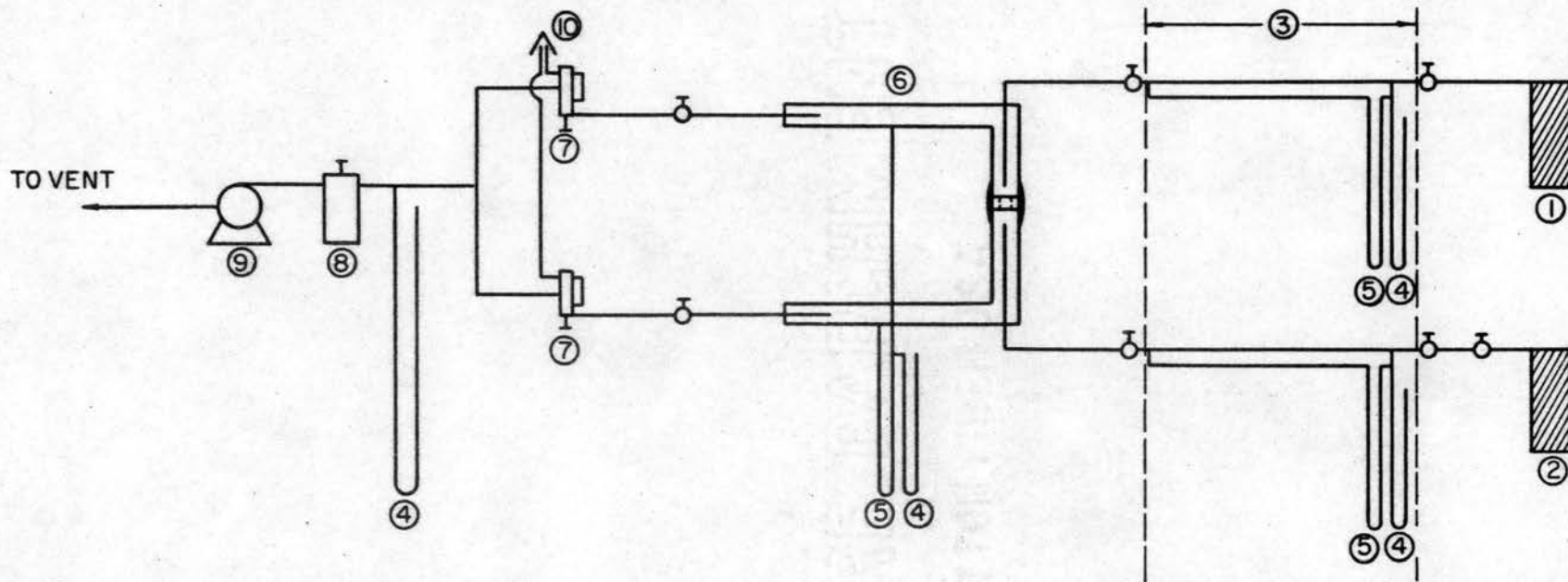
TO VENT

1. C₃H₈ TANK
2. CH₄ TANK
3. CAPILLARY FLOWMETER
4. MERCURY MANOMETER
5. TRIETHYLENE GLYCOL MANOMETER
6. DIFFUSION CELL
7. LINEAR SAMPLE VALVE
8. CARTESIAN MANOSTAT
9. VACUUM PUMP
10. CHROMATOGRAPH INLET

Figure 2. Diagram of the Experimental System
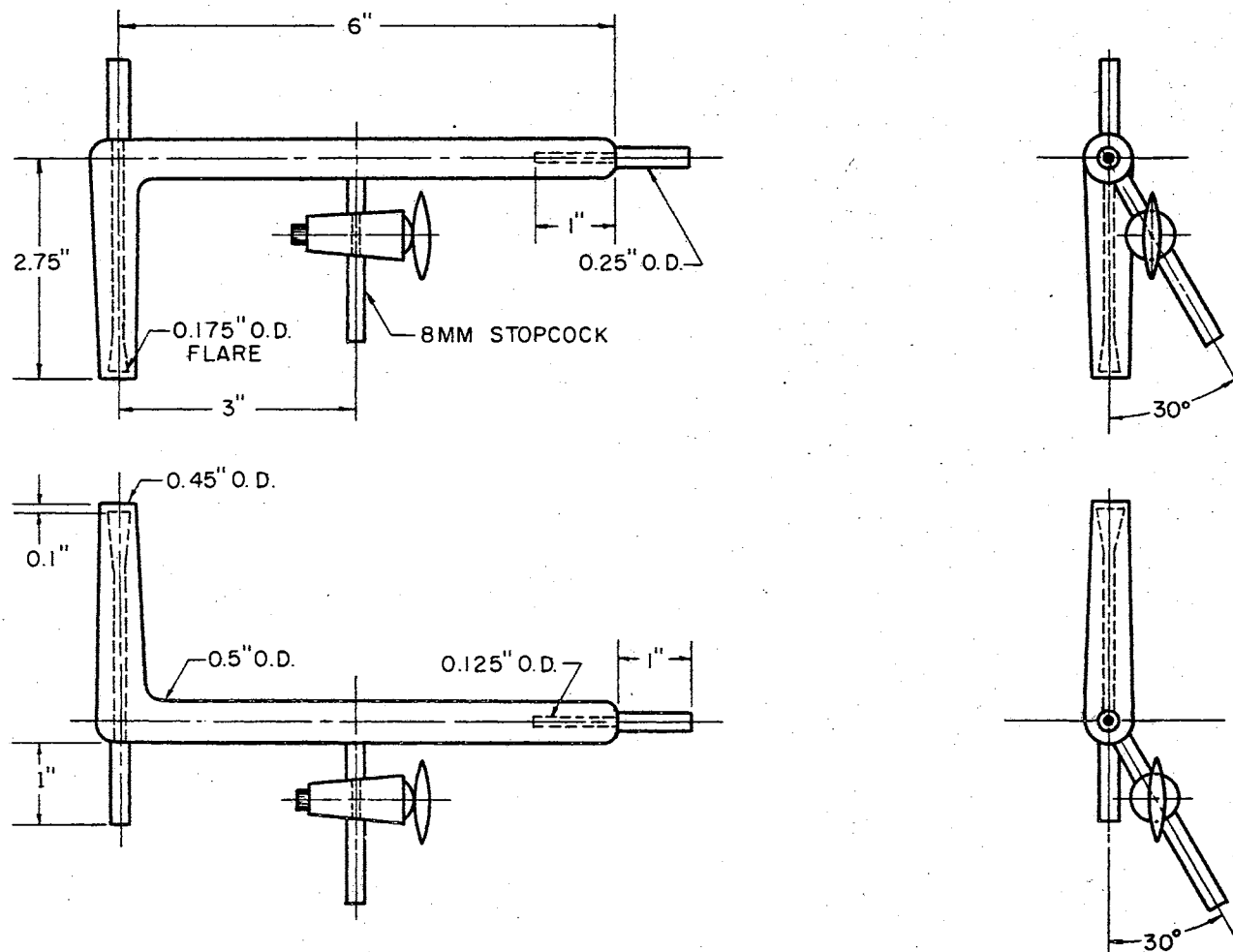
Figure 3. Diffusion Cell -- Details of Glass Parts

Operating Procedure

The object of a run is to determine the actual fluxes for a given pressure, temperature, pellet length, pellet radius, and a set of concentrations at the faces of the pellet. In order to achieve this objective, it is essential that the following procedure be followed. Steps are included in the procedure to prevent the thermoconductivity cell from burning out and to check for leaks within the system.

The first part of the procedure consists of starting the gas chromatograph and reactivating the carbon pellet to be run. The chromatograph is started two days prior to a run to assure that all temperatures reach their steady-state values. All the power in the gas chromatograph except the bridge current is turned on. The helium is turned on and adjusted to a pressure of 38 psi on the inlet pressure gauge of the chromatograph. The flow rates of helium to the chromatograph are adjusted to preset values marked on the rotameters (the number 3 mark). These flow rates had been found to give good separation with the Porapak column packing. After about ten minutes of flushing the system with helium, it is safe to turn on the bridge current which is adjusted to 500 milliamperes. The working temperatures should be $190^{\circ}C$ for the thermoconductivity cell, $150^{\circ}C$ for the column oven, $150^{\circ}C$ for the inlet block, and $220^{\circ}C$ for the outlet block.

While the chromatograph is warming up, the pellet is mounted in its brass ring. This is done by forcing the pellet into the center of the ring which is accurately drilled to match the radius of the pellet. The pellet faces are then carefully filed flat with the surface of the ring. Then the pellet is reactivated to remove any substances it might have adsorbed while being mounted. The pellet and brass ring are placed

in the reactivation bomb connected to the vacuum pump, and placed in an oven. The oven is the one in which the chromatograph columns are located. Vacuum and heat (150°C) are maintained for a period of twenty-four hours. Afterwards the bomb is removed from the oven to cool down to ambient temperature to facilitate handling.

Once cooled, the bomb is disconnected from the vacuum and quickly sealed. The vacuum pump continues to run but is now hooked to the main system. The bomb is quickly opened, the pellet in its ring is mounted in Tygon tubing, and placed in the system. With practice this can all be done in less than five minutes. The system is then kept under vacuum for another three hours to make sure the pellet is degassed as is the rest of the system. This time also allows the pressure on both sides of the pellet to equalize so that the zero point for the differential pressure manometer can be determined. The valves to the vacuum pump are closed and the vacuum pump shut off. The system is left in this condition overnight to check for leaks.

The next morning, the system is ready to run if the vacuum is maintained. First the vacuum pump is restarted and the differential pressure manometer valve closed to prevent an overflow during start up. Then the valves which sealed the system are opened. The three-way stopcocks on the flowmeters are set so that the mercury manometers only are open. The valves at the top of the capillaries are opened about one turn. The tank valves are opened slowly while the regulator valves are left closed. Set the methane outlet pressure at 250 psig and the propane at 0.5 psig. Now open the propane valve fully and just crack the methane regulator valve. On the methane side there are two metering valves before the capillary which are adjusted to allow a small

amount of methane into the system.

The manostat is set to hold an absolute pressure of four inches of mercury. Using the same valves that seal the system, the system pressure is regulated to the desired level. All the time be sure to check the flowmeters to make sure the rates are remaining constant. Now open the differential manometer valve slowly and adjust the flow rates until the pressure differential is zero. Once everything reaches steady-state, the system is allowed to run for twenty minutes before sampling.

After twenty minutes a sample is taken from one side of the diffusion cell and injected into the gas chromatograph. If it is under three mole per cent in the dilute component, the other side is sampled. If the second side is under the desired limit, duplicate samples are taken. If either side is outside the calibration range, the corresponding flow rate is adjusted accordingly and the sampling cycle repeated until both sides are within the limits desired. When the concentrations have been brought within limits, carefully open the TEG manometers to the flowmeters and allow the system to reequilibrate before reading the manometers. Meanwhile check the barometer and temperature. When reading the manometers for the flowmeters the following method of reading must be observed to assure consistent results. All mercury meniscuses are read where they wet the glass and all TEG meniscuses are read at the optical bottom of the concave surface. Once the manometer readings are taken, the run is over.

If enough time remains another run can be taken immediately or if no time is available the system can be shut down for the night. To shut down for the night, first close the tank valves and the valves on the flowmeters, starting with the ones nearest the tanks. Next run the

system up to a high vacuum condition and continue to draw vacuum for about ten minutes. Then seal off the diffusion cell from the vacuum pump. Lastly, shut off the vacuum pump. Leaving the system under vacuum serves two purposes. One is that it checks for minute leaks. Secondly, it leaves the system in condition to start right up the next morning. The chromatograph is allowed to run continuously.

CHAPTER III

DATA AND RESULTS

This investigation was done with Columbia Activated Carbon-Type
NXC 4/6. This is a typical adsorbent for gas processing. It has large
pores (2,000 to 100,000 $\overset{o}{A}$ in diameter) for mass transfer through the
pellet and with small pores (below 18 $\overset{o}{A}$ in diameter) to provide a large
surface area. The physical data for this carbon is shown in Table IX in
Appendix C.

Table I presents the experimental data for the various runs. The
temperature was ambient temperature which is nearly constant in an air-
conditioned laboratory. Pressure varied from 0.137 to 1.002 atmospheres
while the pellet length varied from 0.2515 to 0.3759 centimeters. In
this table, the concentrations are reported as peak height per cents as
explained in Appendix B. The flow rates of pure methane and pure pro-
pane are calculated from the manometer readings as described in Appendix
A.

Table II shows some of the intermediate quantities needed for com-
puting the methane flux with the various theoretical equations. The mole
fractions are those corresponding to the peak height per cents in Table
I and are generally below three mole per cent in the dilute component.
Bulk diffusion coefficients for the methane-propane binary mixture are
calculated by the Wilke-Lee equation (17) with an uncertainty of seven
per cent because so far no one has measured an experimental value for

19

this pair. The procedure is described in Appendix C. The Knudsen diffusion coefficients are found using either Equation (2) or Equation (24) with the overall average pore radius of 7,479.4 $\overset{\text{o}}{\text{A}}$. To convert these coefficients to those for the macro-and micropore regions, all one has to do is to divide by the overall average radius and to multiply by the average radius for the region of interest as given in Table IX. The last two columns show the value of α and the actual methane flux to which the results of the theoretical equations are compared. The value of α is calculated using the actual values of the propane and methane fluxes found using mass balances.

The results for the straight tube models and the Wakao-Smith model are given in Tables III and IV respectively. The values reported are ratios of the calculated methane flux to the actual methane flux since this is the quantity of interest. The difference between the regular and exact equations is the factor $8/3\pi$ which is rounded off to one in the regular equation. For each individual pellet, the average for the runs are shown with the standard deviations. Similarly, the overall averages are shown at the bottom of the columns with the standard deviations for all runs.

Figure 4 is the Rothfeld plot for all three pellets combined. The slope is the tortuosity which equals 11.21 and the intercept equals $1/D_{KA} \sqrt{M_A} = 4.259$. This intercept yields a Knudsen diffusion coefficient of 0.059 cm^2/sec. Using Equation (2) with the calculated value of Knudsen diffusion coefficient, an effective average pore radius of 139.5 $\overset{\text{o}}{\text{A}}$ is calculated.

TABLE I

DATA

Pellet Area = 0.146 cm^2

Run	Temperature ($^\circ$C)	Pressure (atm)	Pellet Thickness (cm)	$\dfrac{\text{Height Methane Peak} \times 100}{\text{Height Methane Peak + Hgt Propane Peak}}$ Methane Rich Stream	Methane Poor Stream	Pure CH$_4$ Flow Rate x 10^3 (g moles/min)	Pure C$_3$H$_8$ Flow Rate x 10^3 (g moles/min)
1	24.5	0.967	0.3556	97.52	2.29	0.978	0.701
2	25.0	0.137	0.3556	95.96	6.60	0.281	0.769
3	25.0	0.311	0.3556	96.67	6.25	0.457	0.698
4	25.0	0.463	0.3556	98.68	6.50	1.168	0.657
5	25.0	0.975	0.3556	97.41	1.42	1.225	0.914
6	26.0	0.142	0.3759	97.74	2.26	0.853	0.891
7	25.3	1.002	0.3759	97.53	1.49	1.054	1.384
8	24.5	0.970	0.3759	97.67	10.07	1.055	0.203
9	25.3	0.990	0.3759	98.55	7.08	1.740	0.370
10	25.0	0.142	0.3759	97.70	2.62	0.731	0.881
11	25.0	0.616	0.3759	98.18	3.63	1.301	0.530
12	24.8	0.139	0.2515	97.12	9.91	0.507	0.327
13	24.8	0.249	0.2515	98.36	2.38	0.913	0.140
14	25.0	0.241	0.2515	98.39	2.43	1.103	1.546
15	25.0	0.595	0.2515	97.69	5.88	0.578	0.737
16	25.5	0.138	0.2515	96.93	4.39	0.437	0.898

TABLE II

INTERMEDIATE QUANTITIES

Run	y_{AO}	y_{AL}	Bulk Diffusion Coefficient (cm^2/sec)	Knudsen Diffusion Coefficients*		Actual**		
				Eq (2) (cm^2/sec)	Deryaguin's Eq (24) (cm^2/sec)	Methane Flux (N_A) (g-moles/cm^2/sec) $\times 10^6$	Propane Flux (N_B) (g-moles/cm^2/sec) $\times 10^5$	$\alpha = 1 - N_B/N_A$
1	0.9785	0.0038	0.132	3.126	2.164	0.295	0.244	-7.27
2	0.9662	0.0090	0.937	3.128	2.166	0.780	0.113	-0.45
3	0.9715	0.0085	0.413	3.128	2.166	0.668	0.151	-1.26
4	0.9883	0.0088	0.278	3.128	2.166	0.650	0.157	-1.41
5	0.9775	0.0020	0.132	3.131	2.168	0.202	0.320	-14.90
6	0.9802	0.003	0.902	3.128	2.166	0.299	0.196	-5.53
7	0.9787	0.002	0.128	3.128	2.165	0.311	0.260	-7.38
8	0.9797	0.0137	0.132	3.128	2.165	0.287	0.248	-7.66
9	0.9866	0.0097	0.130	3.129	2.166	0.386	0.268	-5.95
10	0.9800	0.0035	0.902	3.129	2.166	0.346	0.169	-3.88
11	0.9840	0.0048	0.209	3.131	2.168	0.279	0.240	-7.60
12	0.9752	0.0136	0.932	3.134	2.170	0.494	0.145	-1.95
13	0.9855	0.0329	0.517	3.130	2.167	0.490	0.152	-2.11
14	0.9857	0.0034	0.532	3.126	2.164	0.594	0.181	-2.05
15	0.9799	0.0080	0.216	3.130	2.167	0.665	0.134	-1.01
16	0.9737	0.006	0.930	3.129	2.166	0.609	0.133	-1.17

*Base on Average Radius of 7,479.4Å
**Pellet Area = 0.146 cm^2.

TABLE III

COMPARISON OF DATA WITH STRAIGHT TUBE MODELS

| | N_A (Calculated)/N_A (Actual) | | | |
Run	Regular Equation	Exact Equation	Deryaguin Diffusion Coefficient	Wheeler Diffusion Coefficient
1	5.76	5.77	5.72	5.86
2	4.95	5.11	4.55	6.01
3	5.24	5.31	5.06	5.71
4	5.40	5.45	5.27	5.72
5	5.44	5.45	5.40	5.51
Pellet Ave.	5.36 ± 0.30	5.42 ± 0.24	5.20 ± 0.44	5.77 ± 0.18
6	5.70	5.79	5.44	6.32
7	5.17	5.18	5.13	5.25
8	5.26	5.28	5.23	5.35
9	4.61	4.62	4.57	4.69
10	5.84	5.95	5.55	6.56
11	5.56	5.58	5.50	5.71
Pellet Ave.	5.36 ± 0.45	5.41 ± 0.48	5.24 ± 0.37	5.65 ± 0.39
12	7.92	8.11	7.43	9.14
13	8.06	8.17	7.77	8.81
14	7.04	7.14	6.76	7.74
15	8.31	8.37	8.14	8.72
16	7.54	7.74	7.01	8.87
Pellet Ave.	7.78 ± 0.50	7.91 ± 0.49	7.43 ± 0.56	8.66 ± 0.53
Overall Ave.	6.12 ± 1.22	6.19 ± 1.27	5.91 ± 1.13	6.63 ± 2.26

TABLE IV

COMPARISON OF DATA WITH WAKAO AND SMITH MODEL

	N_A (Calculated)/N_A (Actual)		
Run	Regular Equation	Exact Equation	Deryaguin Diffusion Coefficient
1	1.39	1.42	1.31
2	0.86	0.89	0.74
3	0.97	1.00	0.90
4	1.06	1.09	0.98
5	1.36	1.38	1.29
Pellet Ave.	1.13 ± 0.24	1.16 ± 0.24	1.06 ± 0.23
6	1.04	1.08	0.92
7	1.25	1.28	1.18
8	1.28	1.31	1.21
9	1.10	1.13	1.04
10	1.05	1.09	0.98
11	1.26	1.30	1.18
Pellet Ave.	1.17 ± 0.11	1.20 ± 0.11	1.10 ± 0.11
12	1.39	1.44	1.29
13	1.49	1.54	1.39
14	1.29	1.33	1.20
15	1.66	1.72	1.55
16	1.31	1.36	1.22
Pellet Ave.	1.44 ± 0.15	1.48 ± 0.16	1.34 ± 0.14
Overall Ave.	1.24 ± 0.21	1.28 ± 0.21	1.16 ± 0.20

TABLE V

DATA FOR ROTHFELD CORRELATION

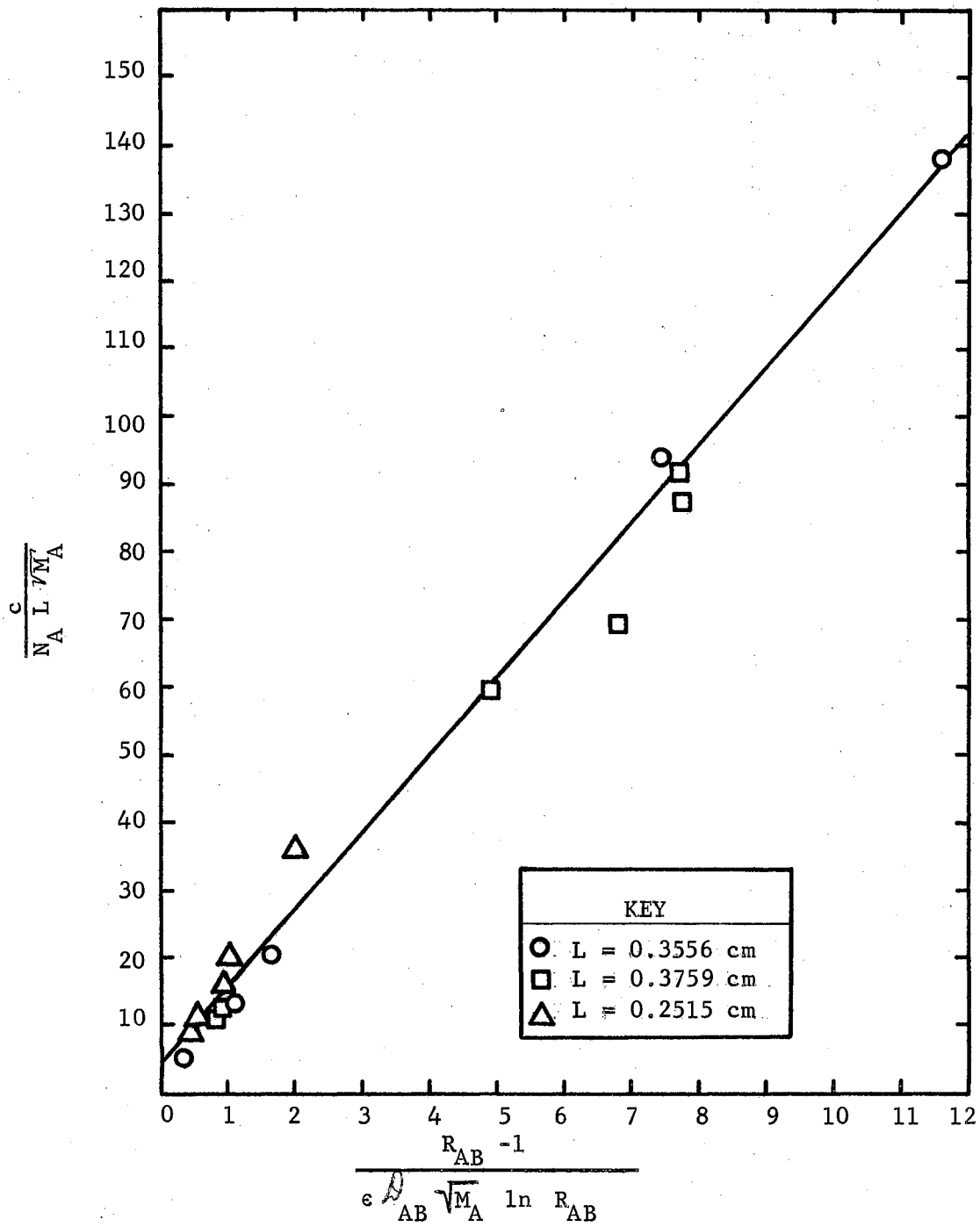| Run	$\dfrac{c}{N_A \, L \, \sqrt{M_A}}$	$\dfrac{R_{AB}-1}{\epsilon \, \lambda_{AB} \, \sqrt{M_A} \, \ln R_{AB}}$	$\dfrac{1}{\lambda_{AB}}$
1	94.16	7.466	7.553
2	5.04	0.371	1.067
3	13.37	1.075	2.423
4	20.42	1.659	3.602
5	138.20	11.687	7.565
6	12.92	0.939	1.109
7	87.66	7.798	7.815
8	91.83	7.708	7.562
9	69.55	6.798	7.709
10	11.16	0.780	1.109
11	59.71	4.850	4.779
12	11.36	0.555	1.073
13	20.57	1.032	1.933
14	16.46	0.993	1.879
15	36.23	1.921	4.624
16	9.19	0.467	1.075

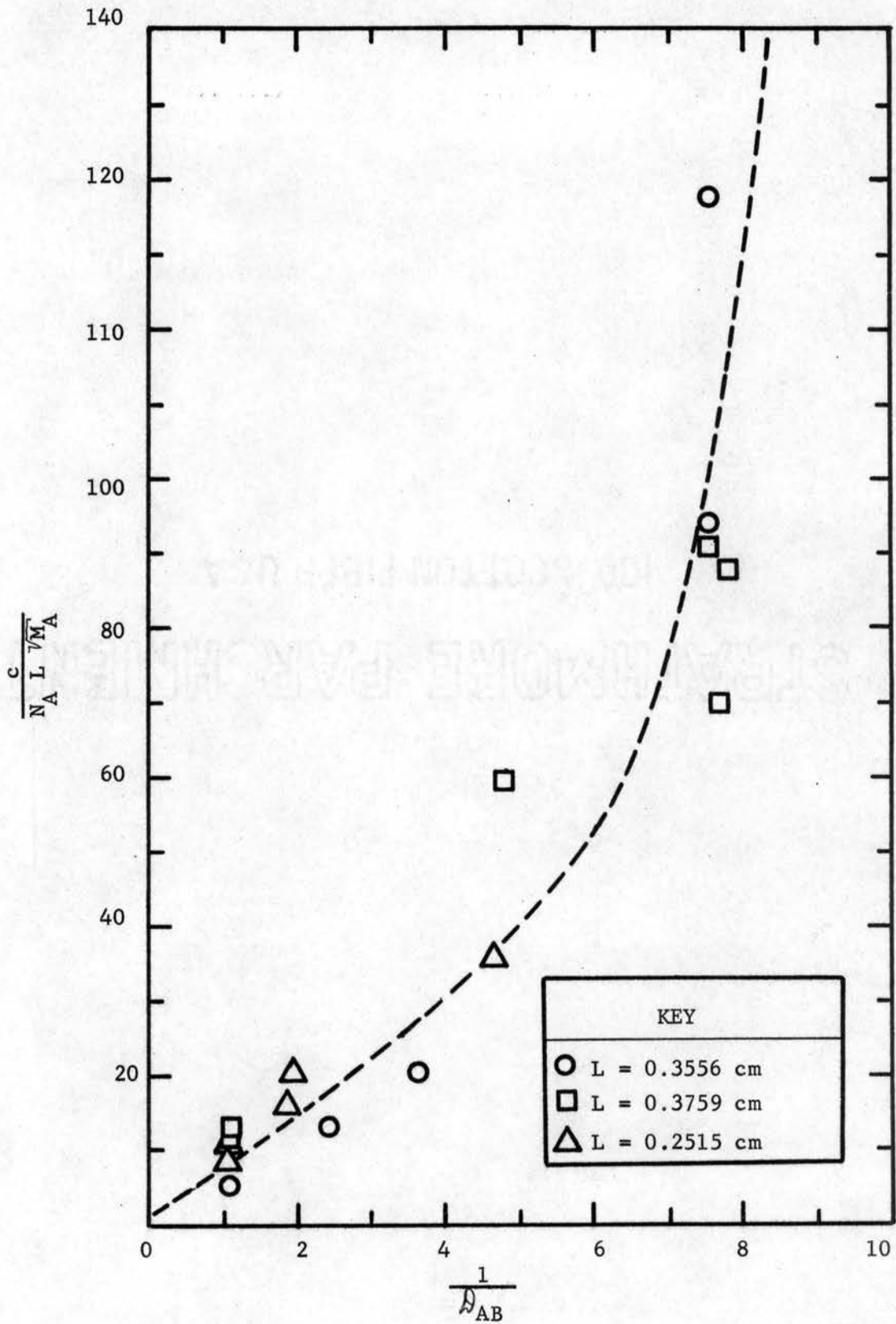Figure 4. Rothfeld Correlation

Figure 5. $\dfrac{c}{N_A\ L\ \sqrt{M_A}}$ vs $\mathcal{D}_{AB}^{-1}$

Discussion

The accuracy of the experimental diffusion fluxes depends on the flow rates of the pure gases and the concentrations of the various streams entering and leaving the diffusion cell. The capillary flow-meters used to measure the flow rates are accurate to $\pm 0.005 \times 10^{-3}$ g-moles/minute. This figure was arrived at through examination of the calibration data. Both incoming pure gases are assumed to contain no impurities since when passed through the gas chromatograph no peaks other than those for the pure gases were noted. The estimated error in composition of the exit streams is ± 0.001 mole fraction. This error is caused mainly by small variations in the sample loop pressure and temperature. An error analysis on the equations for the experimental fluxes show that the probable error in the fluxes is approximately ten per cent.

Good reproducibility of data was observed with newly reactivated pellets as shown by Runs 1 and 7. Consecutive runs also showed good reproducibility as shown by Runs 7 and 8. However, when a run was followed by several runs at higher pressures, and the initial conditions were repeated, the second run showed a smaller flux ratio of propane to methane. Thus Run 6 was followed by Run 10; and Run 12 by Run 16. Since only a limited amount of data was taken, it is hard to pinpoint the cause of this effect which appears to be some type of hysteresis.

Similar effects seemed to take place in Rothfeld's work (8,9) where nitrogen and helium were used with alumina catalyst pellets. His flux ratio varied from 2.30 to 3.25. The concentrations were kept below one per cent on both sides of the pellet. For his argon-helium system the

ratio varied from 3.34 to 4.11. The scatter in both cases is independent of the total pressure. Wakao and Smith (13) also used nitrogen and helium but their ratio varied only from 2.35 to 2.66. Their narrower range might result from working at pressures much above atmospheric pressure. In both cases the investigator was not using a gas that is highly adsorbed.

Both Rothfeld (8) and Dacey (3) attribute the deviation in the flux ratio to the adsorbed layer on the wall. They maintain that the dense layer at the wall ruins the assumptions in the derivation that the collisions with the wall are elastic, specular collisions and that intermolecular collisions and wall collisions contribute equally to the overall momentum transfer. The ratio of the two components is affected by pore distribution, partial pressures, type of porous material involved, etc. Even under steady-state conditions when a particle hits the wall it does not necessarily remove another particle from the same position. This seems reasonable for adsorbed gases since multilayers of the adsorbed phase may be built up.

This leads to another factor which few investigators even mention which is the variation of the thickness of the adsorbed phase along the pore as partial pressure changes. According to Rothfeld (8,9) the plot shown in Figure 5 should be linear if there is no movement on the surface. He does not attempt to say what the relationship should be if movement on the surface does occur. However his plot (8,9) is perfectly linear with a relatively moderate scatter in his flux ratios. Hence, additional factors can be expected to be involved.

The fluxes calculated via the various models contain uncertainities for a number of reasons, namely: Errors in the flux ratio, errors in

bulk diffusion coefficient, errors in the average pore radii. The bulk diffusion coefficient was not known from experimental values so it was necessary to use an empirical equation. The equation used was that of Wilke and Lee (17) which fits the data available in the literature to within seven per cent. The error in the average pore radii is caused by the difficulty in determining the pore radius distribution and the variations of the distribution from pellet to pellet.

Some inaccuracy is also caused by not adjusting the porosities. This would effect the results since tortuosity is a function of porosity (6). Since the Wakao and Smith model has a built-in tortuousity an error is caused by not adjusting the porosities. The Rothfeld model is independent of this error since he uses both a tortuousity and a porosity which can be plotted as a variable ratio.

From Table III, it is readily seen that the straight tube model does not work very well. By comparison, both the Wakao and Smith model displayed in Table IV and the Rothfeld model fit the data reasonably well. The Rothfeld model is easier to apply in that the pore distribution need not be know. Also the equation can be plotted so the slope is equal to q/ϵ. To apply the Wakao and Smith model it is necessary to know the porosity (or densities of the solid and porous material) and the pore distribution. The best results for the Wakao and Smith model are gotten with the Deryaguin Knudsen diffusion coefficient. The only difficulty in applying either model is to know the flux ratio.

CHAPTER IV

SUMMARY

Conclusions

Reliable basic data have been obtained for the diffusional fluxes
of methane and propane in activated carbon. These data show that the
straight tube model is not applicable as was expected. The Rothfeld
and Wakao-Smith models gave results that compare favorably with experi-
mental data. The Rothfeld model yielded a tortuosity of 11.21 while
the Wakao and Smith model with its built-in tortuosity factor fits the
experimental results within an overall average of twenty per cent.
Hence with further refinements as suggested in the next section, both
the Rothfeld and Wakao-Smith models could be used for designing gas
adsorbing equipment for the chemical industry.

Suggestions for Further Work

It is known that the axial porosities vary from the overall porosi-
ties for extruded materials such as used here (6, 16). Hence, the first
thing to try next is to run the same pellets and more of them using a
set of gases which would not be adsorbed by the activated carbon. This
would give some insight into the structure of the pore system. Then by
comparing these results with the results for the methane-propane system
plus the results for methane and propane each paired with one of the

31

non-adsorbed gases some idea about the effect of the binary adsorbed layer. To damp out any variations from pellet to pellet it is suggested that the diffusion cell be modified so that more than one pellet can be used at one time.

Adsorption studies should be carried out with both the pure gases and with various mixture of both. From this data, surface diffusion coefficients can be calculated for the pure gases and maybe a binary surface diffusion coefficient can be found. This might be a function of the pore structure so it should be done for more than one type of material.

To generalize the theory, materials of various pore structures, lengths, pellet radii, and adsorption capacity should be run. These generalizations should also give some insight into what causes the flux ratio to vary from the theoretical values.

Since unsteady-state is the one which usually occurs in industrial processes it should also be investigated. These studies would give data on the effect of dead end pores and surface roughness to which steady-state studies are insensitive (6).

Finally, Equation (27) should be tried as a porous material equation as suggested in the text. Also to be tried is a model similar to Rothfeld's. The difference being that the new model would use a Wheeler effective diffusion coefficient. This new model is

$$(N_A)_{TOTAL} = (N_A)_{KNUDSEN} + (N_A)_{BULK} \qquad (29)$$

or

$$N_A RTL/P = \frac{\overline{D}_{KA}\, \epsilon}{q}\, (y_{AL} - y_{AO}) + \frac{\mathcal{D}_{AB}\, \epsilon}{q}\, (1 - \exp\, (-\frac{\overline{D}_{KA}\, q}{\epsilon \mathcal{D}_{AB}}))\ln \frac{1 - \alpha y_{AL}}{1 - \alpha y_{AO}} \qquad (30)$$

This equation could also be used for the Wakao and Smith model if someone wishes to solve the difficult integration problem.

SELECTED BIBLIOGRAPHY

(1) Basic Concepts of Adsorption on Activated Carbon. Pittsburg
       Activated Carbon Company, Pittsburg, Pa. (1962).

(2) Bird, R. B., W. E. Stewart, and E. N. Lightfoot, Transport
       Phenomena. John Wiley and Sons, Inc., New York, N. Y.
       (1962).

(3) Dacey, J. R., "The Interface Symposium-10." Ind. and Eng. Chem.
       Vol. 57. (1965) 30.

(4) Enneking, J. C., Personal Communication. January, 1966.

(5) McGlasnan, M. L. and D. J. B. Potter, "The Second Virial Coefficients
       of Some n-Alkanes." Proceedings of the 1958 Joint Conference
       on Thermodynamics and Transport Properties of Fluids-Institute
       of Mechanical Engineers (1958) 60.

(6) Peterson, E. E., Chemical Reaction Analysis. Prentice-Hall, Inc.
       Englewood Cliffs, N. J. (1965).

(7) Present, R. D., Kinetic Theory of Gases. McGraw-Hill Book Company,
       Inc., New York, N. Y. (1955).

(8) Rothfeld, L. B., Diffusion and Flow of Gases in Porous Catalyst.
       Ph.D. dissertation, University of Wisconsin (1961).

(9) Rothfeld, L. B., "Gaseous Counterdiffusion in Catalyst Pellets."
       A. I. Ch. E. Journal Vol. 9 (1963) 19.

(10) Scheidegger, A. E., Physics of Flow Through Porous Media. MacMillan
       Company, New York, N. Y. (1960).

(11) Scott, D. S. and F. A. L. Dullien, "Diffusion of Idea Ideal Gases in
       Capillaries and Porous Solids." A. I. Ch. E. Journal Vol. 8.
       (1962) 113.

(12) Scott, D. S. and F. A. L. Dullien, "The Flow of Rarefied Gases."
       A. I. Ch. E. Journal Vol. 8. (1962) 293.

(13) Wakao, N. and J. M. Smith, "Diffusion in Catalyst Pellets."
       Chemical Engineering Science Vol. 17. (1962) 825.

(14) Wakao, N., S. Otani and J. M. Smith, "Significance of Pressure
       Gradients in Porous Materials." A. I. Ch. E. Journal Vol. 11
       (1965) 435.

(15) Wakao, N., M. R. Rao and J. M. Smith, "Diffusion and Reaction Rates
          in the Ortho-Hydrogen Conversion." Ind. Eng. Chem. Fund.
          Vol. 3. (1964) 127.

(16) Weiz, P. B., "Diffusivity of Porous Particles." Zeitschrift für
          Physikalische Chemie, Bond 11, (1957) 1.

(17) Wilke, C. R. and C. Y. Lee, "Estimation of Diffusion Coefficients
          of Gases and Vapors." Ind. and Eng. Chem. Vol. 47. (1955)
          1253.

APPENDIX A

FLOWMETER CALIBRATION

The capillary flowmeter was calibrated using a bubble flowmeter whose volume was measured using pure water. The results were then plotted as a modified Hagen-Poiseuille Equation.

The form of the Hagen-Poiseuille Equation modified was

$$W = \pi \Delta p \bar{r}_c^{\,4} \rho / (8\mu \, LZ) \tag{31}$$

It is possible to neglect the effect of varying compressibility of the gas since the range of operation is near one atmosphere and below where Z is nearly equal to one and varies very slowly. The true capillary radius is unknown but a constant as is the length. Thus they both can be incorporated with Z into a constant factor.

A Z nearly equal to one implies that the Ideal Gas Law can be used to approximate the density of the gas. Along these same lines, the viscosity is represented as the square root of the ratio of ambient temperature to the reference temperature (22.0°C) times a constant. This comes from the theory of gases composed of hard spheres. Thus the need of good data on viscosity and density is removed allowing the Hagen-Poiseuille Equation to be reduced to

$$W = K\bar{p} \, \Delta p / (T\sqrt{T/T_R}) \tag{32}$$

where K contains everything that remains constant.

Since Δp is read from a U-tube manometer, the conversion factor for

converting the height differential to pressure differential is incorpo-

rated into the constant. Thus Equation (32) becomes

$$W = K' \, \bar{p} \, \Delta h / (T\sqrt{T/T_R}) \tag{33}$$

Therefore by plotting molal flowrate versus $\bar{p} \, \Delta h / (T\sqrt{T/T_R})$, the value

of K' can be determined. This will be true only if the bore of the

capillary is reasonably consistent. Also the intercept should be

zero.

The two resulting equations were

$$W = \bar{p} \, \Delta h / (2013T\sqrt{T/T_R}) \tag{34}$$

for methane and

$$W = \bar{p} \, \Delta h / (1395T\sqrt{T/T_R}) \tag{35}$$

for propane.

TABLE VI

DATA FOR METHANE FLOWMETER

$W \times 10^3$ (moles/min)	P_{HIGH} (In. of Hg)	Δh (In. of triethylene glycol)	T ($^\circ K$)	$\frac{\bar{p}}{T} \frac{\Delta h}{(T/T_R)^{\frac{1}{2}}}$
0.2381	29.74	4.73	296.0	0.475
0.9058	30.79	16.85	294.0	1.805
0.8675	30.80	16.34	294.0	1.742
0.9774	30.82	18.19	294.0	1.952
0.6847	30.49	13.13	295.0	1.380
1.0516	30.64	20.32	295.5	2.543
0.8655	30.49	16.78	295.5	1.741
1.2884	31.01	24.25	295.5	2.609
0.5795	30.07	11.20	296.0	1.152
0.2739	29.48	5.54	296.0	0.554
0.2565	29.62	5.07	296.0	0.509
0.2559	29.61	5.09	295.0	0.513
0.8612	30.44	16.33	295.0	1.712
1.4513	31.26	26.76	295.0	2.918
1.3445	31.15	24.91	295.0	2.707
0.9290	30.63	17.67	296.0	1.862
1.0833	30.81	20.52	296.0	2.179
1.1774	30.83	22.42	296.0	2.385
1.2400	30.00	22.87	299.0	2.357
1.1512	30.56	22.53	303.0	2.300
1.2051	30.79	23.50	303.5	2.421
1.2090	30.74	23.65	304.0	2.428
1.2562	31.02	23.39	296.0	2.515
1.3173	31.14	24.58	296.0	2.653
0.0987	29.57	2.01	296.5	0.199

TABLE VII

DATA FOR PROPANE FLOWMETER

$W \times 10^3$ (moles/min)	P_{HIGH} (In. of Hg)	Δh (In. of triethylene glycol)	T (°K)	$\dfrac{\bar{p} \; \Delta h}{T} (T/T_R)^{\frac{1}{2}}$
1.540	31.99	20.41	294.0	2.166
1.217	31.43	16.23	294.5	1.695
1.377	31.65	18.30	294.5	1.919
1.039	31.14	13.96	294.5	1.448
0.771	30.64	10.38	294.5	1.065
0.573	30.13	7.85	294.5	0.794
1.083	31.17	14.72	296.0	1.517
0.793	30.70	10.87	296.0	1.109
0.2897	29.81	4.06	296.0	0.406

APPENDIX B

CHROMATOGRAPH CALIBRATION

The gas chromatograph was calibrated using standardized samples supplied by Continental Oil Company. The concentrations sent with the samples were those from their runs on their own gas chromatograph which is calibrated using peak heights. The bomb containing the standardized gas is connected to the sampling valve which would be used for that particular mixture in the diffusion runs. Before the bomb is opened to the system, the control manostat is set to four inches of mercury absolute pressure. Next, the bomb valve is barely cracked and the mixture allowed to flow through the system for about ten minutes. Now the samples for calibration. Five samples are taken and the average value of the ratio of the peak height of the dilute component to the sum of the peak heights is plotted against the concentration of the dilute component. The coordinates for the dilute propane samples are converted to data for methane. The resulting curve is nearly linear and is reproducible from day to day as long as the absolute pressure in the sampling valve is kept at four inches of mercury and the chromatograph parameters are left unchanged.

TABLE VIII

CHROMATOGRAPH CALIBRATION DATA

Column Temperature = 150°C

Thermoconductivity Cell Temperature = 190°C

Sample Loop Pressure = 4 inches (absolute) Hg

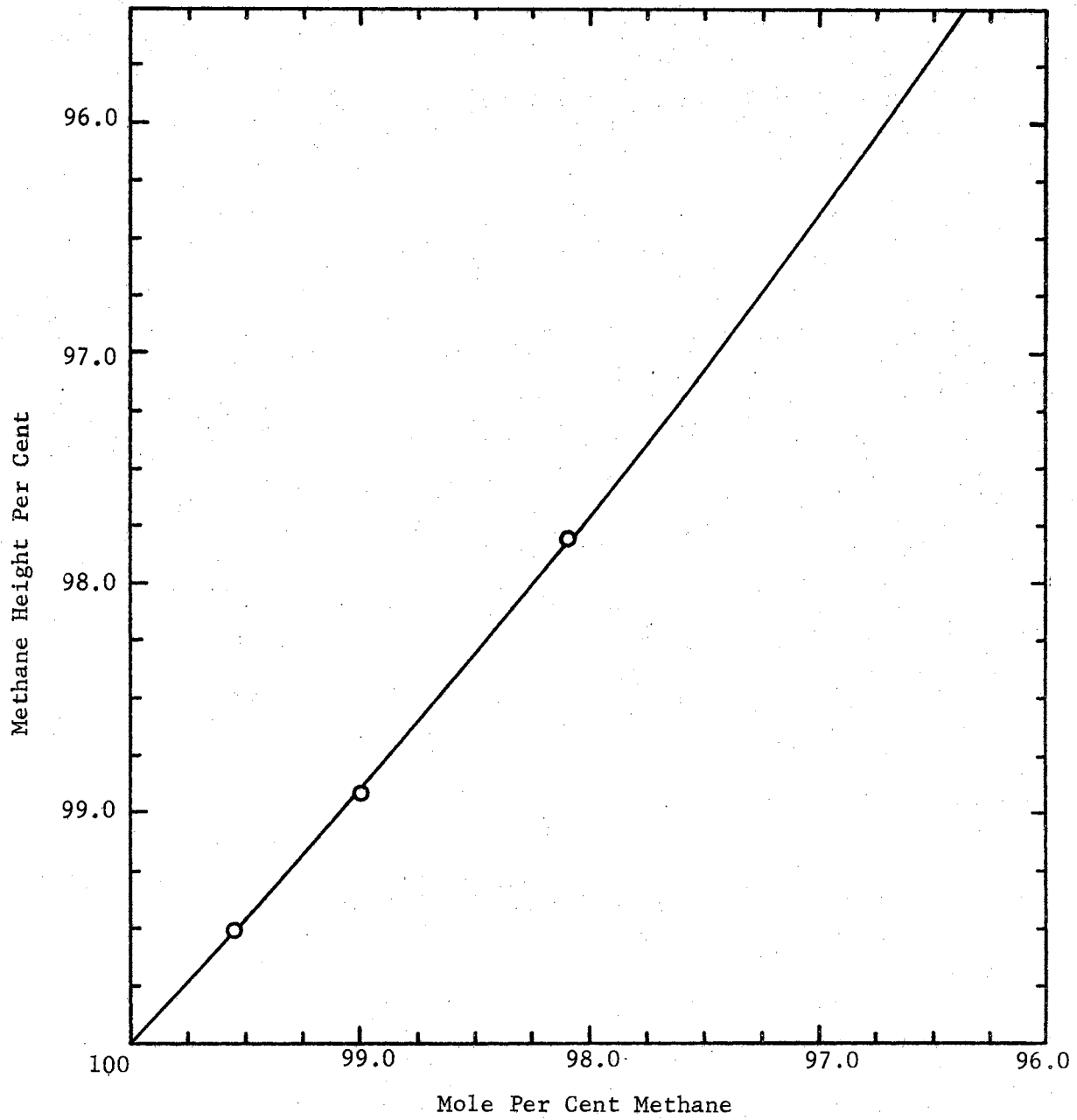| Sample	Actual Concentration of Methane	Average Height Methane (inch)	Average Height Propane (inch)	Methane Height Per Cent
KC-1	0.9954	8.84	0.045	99.494
KC-2	0.9900	9.02	0.100	98.904
KC-3	0.9809	8.70	0.195	97.808
KC-4	0.0051	0.32	8.05	3.82
KC-5	0.0118	0.70	7.70	8.33
KC-6	0.0373	2.41	6.68	26.51

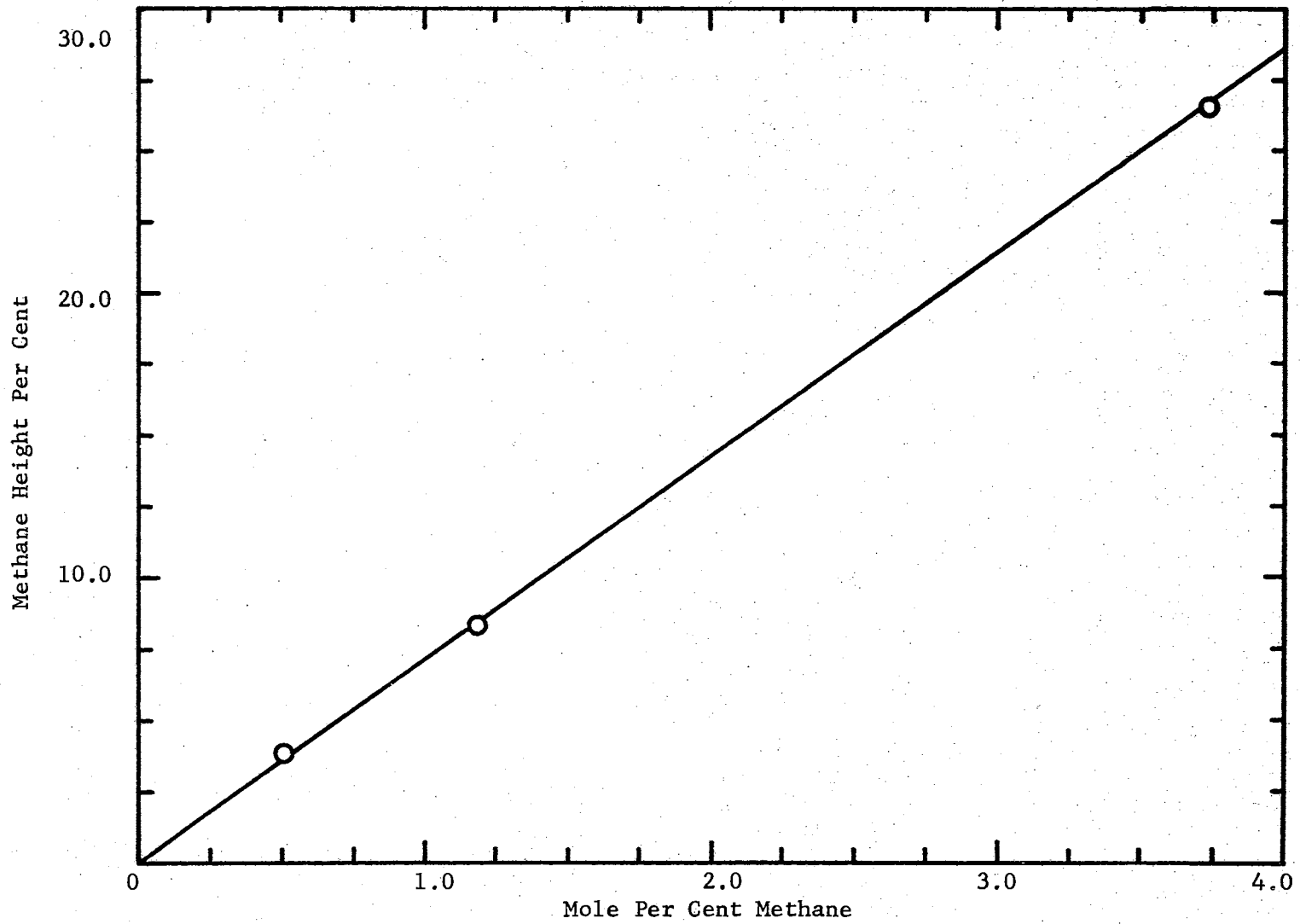Figure 6. Calibration Curve for Methane-Rich Stream

Figure 7.   Calibration Curve for Methane-Poor Stream

APPENDIX C

SAMPLE CALCULATIONS

Most of the calculations involved in this study just involve putting the experimental data into the various equations. However, $\mathcal{D}_{AB}$, the various radii, and the various fluxes must be calculated. For $\mathcal{D}_{AB}$ the Wilke-Lee correlation (17) is used. Their correlation is

$$\mathcal{D}_{AB} = \frac{(10.7 - 2.46(M_A^{-1} + M_B^{-1})^{\frac{1}{2}})10^{-4} \; T^{3/2} (M_A^{-1} + M_B^{-1})^{\frac{1}{2}}}{P \; \sigma_{AB}^2 \; \Omega_{\mathcal{D}}} \tag{36}$$

where $\sigma_{AB} = \frac{1}{2} (\sigma_A + \sigma_B)$

For the methane-propane system $\Omega_{\mathcal{D}}$ can be well represented by

$$\Omega_{\mathcal{D}} = 0.825 - 0.8093T \; 10^{-3} \tag{37}$$

over the narrow range of temperatures used.

The average pore radii are found using integral averages if a suitable distribution is available. However the pore distribution supplies with the Columbia Activated Carbon (Figure 8) is not suitable hence the integrals were converted to summations as follows

$$\bar{r} = \sum_i \bar{r}_i \; V_i / \sum_i V_i \tag{38}$$

The summation covers the range of pore radii desired. The division between macro and micro regions occurs at a pore radius of 500 Angstroms (1). All pores of radius less than nine Angstroms were neglected and the various porosities adjusted. This was done because the exact sizes were not known. It is assumed that they contribute nothing to the diffusion

44

flux. The macroporosity and the microporosity are found by

$$\epsilon_i = \epsilon_{ws} \, V_i / V_{DIFF} \tag{39}$$

$$\epsilon_a = \epsilon_{ws} - \epsilon_i \tag{40}$$

$$\text{where } \epsilon_{ws} = \epsilon \, V_{DIFF} / V_{TOTAL} \tag{41}$$

The fluxes are found by taking a mass balance around the diffusion cell. The mass balance is set up on the computer so that it is necessary only to supply inlet and outlet concentrations in addition to the flowmeter data. Also the outlet concentrations are assumed to be those in contact with the faces of the pellet. The following computer program was used to carry out the various calculations.

```
ISN          SOURCE STATEMENT

  0  $IBFTC          NODECK
     C      PROGRAM FOR CALCULATING DIFFUSIONAL FLUXES IN POROUS MATERIAL
  1          DIMENSION Z(10),YAL(10),F(10),YAC(10),T(10),P(10),R(10),ANA(10),AN
            1B(10),ALPHA(10),DAB(10),DKFB(10),DKIB(10),RATE(10),RATI(10),ANO(10
            2),AN1(10),AN2(10),AN3(10),T0(10),T1(10),T2(10),T3(10),DKFI(10),DKF
            3A(10),DKII(10),DKIA(10),U1(10),U2(10),U3(10),U4(10),ANO1(10),ANO2(
            410),ANO3(10),ANOT(10),AN11(10),AN12(10),AN13(10),AN1T(10),AN21(10)
            5,AN22(10),AN23(10),AN2T(10),AN31(10),AN32(10),AN33(10),AN3T(10),T0
            6B(10),T1B(10),T2B(10),T3B(10),P1(10)
  2          DIMENSION PC01(10),PC02(10),PC03(10),PC11(10),PC12(10),PC13(10),PC
            121(10),PC22(10),PC23(10),PC31(10),PC32(10),PC33(10)
  3          DIMENSION ANOW(10),AN3W(10),TOW(10),T3W(10),ANOW1(10),ANOW2(10),AN
            1OW3(10),ANOWT(10),AN3W1(10),AN3W2(10),AN3W3(10),AN3WT(10)
  4          DIMENSION PC01W(10),PC02W(10),PC03W(10),PC31W(10),PC32W(10),PC33W(
            110),ANOTW(10),AN3TW(10),TOBW(10),T3BW(10)
  5          DIMENSION A1(10),A2(10),PATM(10),PHGM(10),PHGB(10),DTEGM(10),DTEGB
            1(10),PBARM(10),PBARB(10),B(6),ANOW4(10),TOW4(10)
  6  100 FORMAT(I3)
  7          READ(5,100) K
 11          DO 25 J=1,K
     C      STRAIGHT TUBE MODEL
 12    1 FORMAT(F7.4,3E10.0,F8.5,2I2)
 13          READ(5,1)POR,FB,RMAC,RMIC,DP,N,M
 16          A=(3.14159*(DP**2))/4.
 17    2 FORMAT(2F8.5/(4E18.5))
 20          READ(5,2)YAO,YBO,(YAL(I),YAC(I),I=1,N)
 25    3 FORMAT(2F7.4/(3E7.4))
 26          READ(5,3)PORA,PORI,(T(I),P(I),R(I),I=1,N)
 33    4 FORMAT(5F14.5)
 34          READ(5,4)(PATM(I),PHGM(I),DTEGM(I),PHGB(I),DTEGB(I),I=1,N)
 41          DO20 I=1,N
 42          PBARM(I)=PATM(I)+(PHGM(I)/2.54)-.5*(DTEGM(I)/2.54*.0829
 43          PBARB(I)=PATM(I)+(PHGB(I)/2.54)-.5*(DTEGB(I)/2.54*.0829
 44          IF(M)51,52,52
 45   51 F(I)=PBARB(I)*(DTEGB(I)/2.54)/(1395.*T(I)*(T(I)/295.)**.5)
 46          GO TO 53
 47   52 F(I)=PBARB(I)*(DTEGB(I)/2.54)/(786.*T(I)*(T(I)/295.)**.5)
 50   53 Z(I)=PBARM(I)*(DTEGM(I)/2.54)/(2013.*T(I)*(T(I)/295.)**.5)
 51          YAB=1.-YBO
 52          CD=YAC(I)-YAL(I)
 53          G=(Z(I)*(YAO-YAL(I))+F(I)*(YAB-YAL(I)))/(60.*CD)
 54          D=(Z(I)*(YAC(I)-YAO)+F(I)*(YAC(I)-YAB))/(60.*CD)
 55          ANAB=Z(I)*YAO/60.-G*YAC(I)
 56          ANBB=F(I)*YBO/60.-D*(1.-YAL(I))
 57          ANA(I)=ANAB/A
 60          ANB(I)=ANBB/A
 61          ALPHA(I)=1.-ANB(I)/ANA(I)
 62          P1(I)=P(I)/29.92
 63          IF(M)5,5,6
 64    5 SS=19.99431
 65          BET=1.651-.0016187*T(I)
 66          BA=9.983E-04*2.
 67          AM=.29159
 70          GO TO 23
 71    6 SS=19.70916
```

ISN		SOURCE STATEMENT
72		BET=1.855-.0017941*T(I)
73		BA=10.006E-04*2.
74		AM=.28206
75	23	DAB(I)=BA*T(I)**1.5*AM/(P1(I)*SS*BET)
76		Y=SQRT(13199144.*T(I))
77		DKFB(I)=.666667*FB*Y
100		DKIB(I)=.461539*FB*Y
101		DA=P1(I)*DAB(I)/(82.057*T(I)*R(I)*ALPHA(I))
102		DD=POR*DA
103		RT=1.-YAL(I)*ALPHA(I)
104		RB=1.-YAC(I)*ALPHA(I)
105		RATE(I)=DAB(I)/DKEB(I)
106		RATI(I)=DAB(I)/DKIB(I)
107		ANO(I)=DD*ALOG((RT+RATE(I))/(RB+RATE(I)))
110		AN1(I)=DD*ALOG((RT+.84882638*RATE(I))/(RB+.84882638*RATE(I)))
111		AN3(I)=DD*ALOG((RT+RATI(I))/(RB+RATI(I)))
112		TO(I)=ANO(I)/ANA(I)
113		T1(I)=AN1(I)/ANA(I)
114		T3(I)=AN3(I)/ANA(I)
115		D6=ALOG(RT/RB)
116		DKEI(I)=.666667*RMIC*Y
117		DKEA(I)=.666667*RMAC*Y
120		DKII(I)=.461539*RMIC*Y
121		DKIA(I)=.461539*RMAC*Y
122		B(1)=-DKEB(I)/DAB(I)
123		B(2)=-DKIB(I)/DAB(I)
124		B(3)=-DKEA(I)/DAB(I)
125		B(4)=-DKEI(I)/DAB(I)
126		B(5)=-DKIA(I)/DAB(I)
127		B(6)=-DKII(I)/DAB(I)
130		ANOW(I)=DD*(1.-EXP(B(1)))*D6
131		AN3W(I)=DD*(1.-EXP(B(2)))*D6
132		ANOW4(I)=DD*ALOG((1./(1.-EXP(B(1)))-YAL(I)*ALPHA(I))/(1./(1.-EXP(B 1(1)))-YAC(I)*ALPHA(I)))
133		TOW(I)=ANOW(I)/ANA(I)
134		T3W(I)=AN3W(I)/ANA(I)
135		TOW4(I)=ANOW4(I)/ANA(I)
C		BIDISPERSED MODEL
136		U1(I)=DAB(I)/DKEI(I)
137		U2(I)=DAB(I)/DKEA(I)
140		U3(I)=DAB(I)/DKII(I)
141		U4(I)=DAB(I)/DKIA(I)
142		DB=((1.-PORA)/PORI)**2
143		D1=DAB(I)*(DB+RMIC/RMAC)/(DKEI(I)*(1.+DB))
144		D2=DAB(I)*(DB+RMIC/RMAC)/(DKII(I)*(1.+DB))
145		D3=PORA**2
146		D4=PORI**2
147		ANO1(I)=DA*D3*ALOG((RT+U2(I))/(RB+U2(I)))
150		AN11(I)=DA*D3*ALOG((RT+.84882638*U2(I))/(RB+.84882638*U2(I)))
151		AN31(I)=DA*D3*ALOG((RT+U4(I))/(RB+U4(I)))
152		AN72(I)=DA*D4*ALOG((RT+U1(I))/(RB+U1(I)))
153		AN12(I)=DA*D4*ALOG((RT+.84882638*U1(I))/(RB+.84882638*U1(I)))
154		AN32(I)=DA*D4*ALOG((RT+U3(I))/(RB+U3(I)))
155		D5=4.*PORA*(1.-PORA)/(1.+DB)
156		ANO3(I)=DA*D5*ALOG((RT+D1)/(RB+D1))

ISN	SOURCE STATEMENT
157	AN13(I)=DA*D5*ALOG((RT+.84882638*D1)/(RB+.84882638*D1))
160	AN33(I)=DA*D5*ALOG((RT+D2)/(RB+D2))
161	ANOT(I)=ANO1(I)+ANO2(I)+ANO3(I)
162	AN1T(I)=AN11(I)+AN12(I)+AN13(I)
163	AN3T(I)=AN31(I)+AN32(I)+AN33(I)
164	TOB(I)=ANOT(I)/ANA(I)
165	T1B(I)=AN1T(I)/ANA(I)
166	T3B(I)=AN3T(I)/ANA(I)
167	PCO1(I)=ANO1(I)/ANOT(I)
170	PCO2(I)=ANO2(I)/ANOT(I)
171	PCO3(I)=1.-PCO1(I)-PCO2(I)
172	PC11(I)=AN11(I)/AN1T(I)
173	PC12(I)=AN12(I)/AN1T(I)
174	PC13(I)=1.-PC11(I)-PC12(I)
175	PC31(I)=AN31(I)/AN3T(I)
176	PC32(I)=AN32(I)/AN3T(I)
177	PC33(I)=1.-PC31(I)-PC32(I)
200	ANOW1(I)=DA*D3*(1.-EXP(B(3)))*D6
201	ANOW2(I)=DA*D4*(1.-EXP(B(4)))*D6
202	AN3W1(I)=DA*D3*(1.-EXP(B(5)))*D6
203	AN3W2(I)=DA*D4*(1.-EXP(B(6)))*D6
204	ANOW3(I)=DA*PORA*(1.-PORA)*(1.-EXP(B(3)))*(1.-EXP((1.-EXP(B(4))))/(
	1DB*(1.-EXP(B(3))))))*D6*2.
205	AN3W3(I)=DA*PORA*(1.-PORA)*(1.-EXP(B(5)))*(1.-EXP((1.-EXP(B(6))))/(
	1DB*(1.-EXP(B(5))))))*D6*2.
206	ANOWT(I)=ANOW1(I)+ANOW2(I)+ANOW3(I)
207	AN3WT(I)=AN3W1(I)+AN3W2(I)+AN3W3(I)
210	PCO1W(I)=ANOW1(I)/ANOWT(I)
211	PCO2W(I)=ANOW2(I)/ANOWT(I)
212	PCO3W(I)=1.-PCO1W(I)-PCO2W(I)
213	PC31W(I)=AN3W1(I)/AN3WT(I)
214	PC32W(I)=AN3W2(I)/AN3WT(I)
215	PC33W(I)=1.-PC31W(I)-PC32W(I)
216	TOBW(I)=ANOWT(I)/ANA(I)
217	T3BW(I)=AN3WT(I)/ANA(I)
220	A3=SQRT(16.04)
221	A1(I)=P1(I)/(82.057*T(I)*ANA(I)*R(I)*A3)
222	20 A2(I)=(ANB(I)/ANA(I)-1.)/(POR*DAB(I)*A3*ALOG(ANB(I)/ANA(I)))

TABLE IX

PHYSICAL DATA

Columbia Activated Carbon-Type NXC 4/6

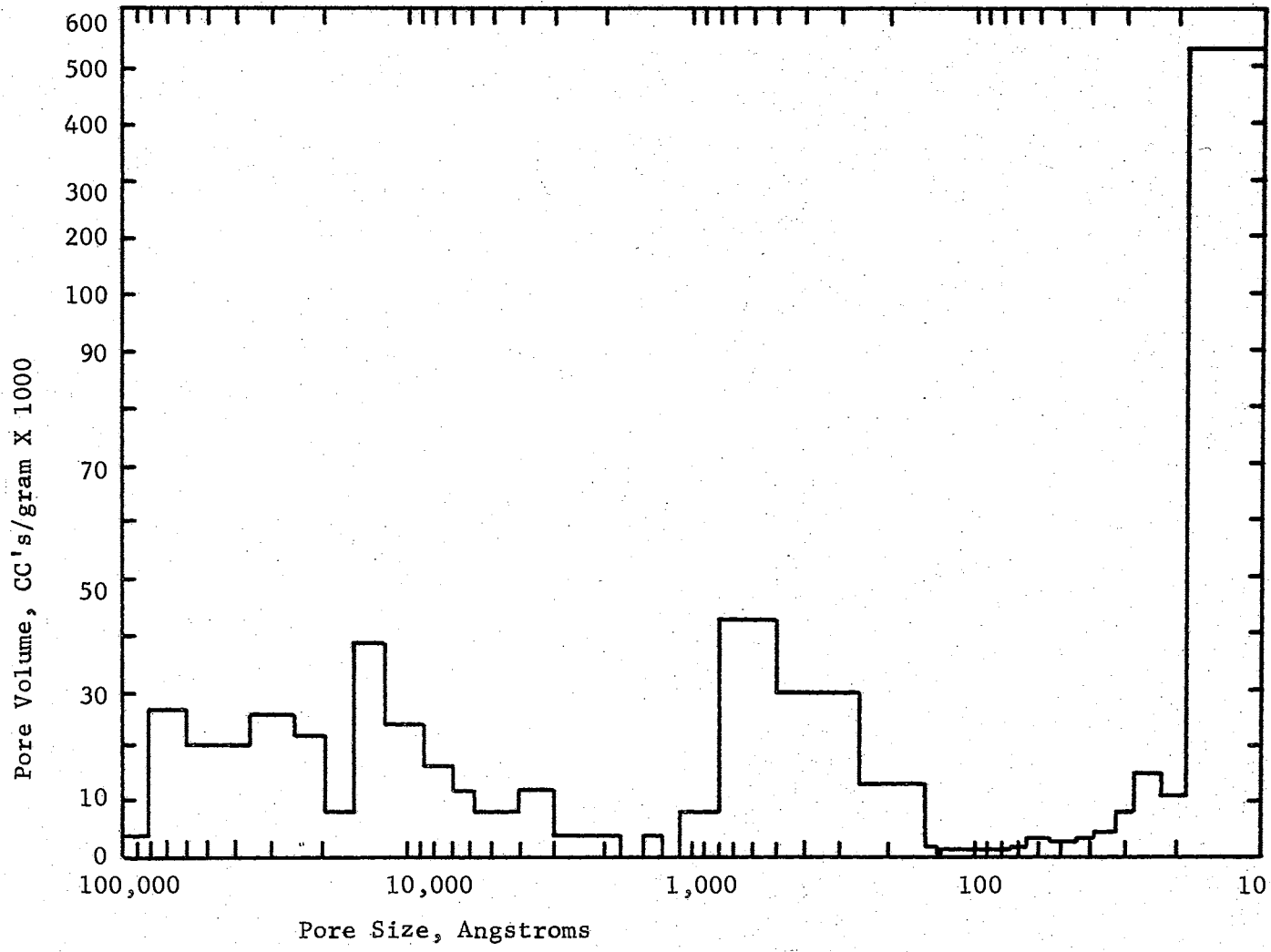|	
ϵ (from Columbia Carbon Co.)	0.869
ϵ (neglecting pores of $r < 9\ \overset{o}{A}$)	0.413
ϵ_i ($r < 500\ \overset{o}{A}$)	0.169
ϵ_a ($r > 500\ \overset{o}{A}$)	0.244
$\bar{r}$	7,479.4 $\overset{o}{A}$
$\bar{r}_i$	175.82 $\overset{o}{A}$
$\bar{r}_a$	12,503.9 $\overset{o}{A}$
Pellet Area of Axial Face	0.146 cm^2
Internal Surface Area (from Columbia Carbon Co.)	approx. 1,200 m^2/g

Figure 8. Pore Size Distribution (Columbia Carbon Company)

NOMENCLATURE

(L = Length, M = Mass, T = Temperature, t = time)

Symbol	Quantity	Dimensions
c	Concentration	$(moles/L^3)$
$\mathcal{D}_{AB}^{K}$	Knudsen Diffusion Coefficient Eq. (14)	(L^2/t)
D_{AB}	Overall Diffusion Coefficient Eq. (16)	(L^2/t)
$\mathcal{D}_{AB}$	Binary Bulk Diffusion Coefficient	(L^2/t)
$\overline{D}_{KA}$	Knudsen Diffusion Coefficient for Some Average Property Eq. (2)	(L^2/t)
$\overline{D}_{DKA}$	Deryaguin's Knudsen Diffusion Coefficient	(L^2/t)
$\vec{J}_A$	Molar Flux Relative to Molar Average Velocity	$(moles/L^2 - t)$
K, K'	Constants	
k	Bolzmann Constant	$(ML^2/t^2 T \text{ molecule})$
L	Geometric Length	(L)
M	Mole Weight	(M/mole)
m	Molecular Weight	(M/molecule)
N	Molar Flux Relative to Laboratory Coordinates	$(moles/L^2 t)$
n	Molecular Density	$(molecules/L^3)$
P, $\overline{p}$	Total Pressure	$(atm \text{ and } M/L^2)$
p	Partial Pressure	$(atm \text{ and } M/L^2)$
Q	N_A (Calculated)$/N_A$ (Actual)	

Nomenclature (Continued)

Symbol	Quantity	Dimensions
q	Rothfeld Tortuosity Factor	
R	Ideal Gas Law Constant	$\left(\dfrac{ML^2}{t^2 \text{ g-mole } T}\right)$
		or $\left(\dfrac{\text{ATM } L^3}{\text{g-mole } T}\right)$
R_{AB}	$|N_B/N_A|$	
$\bar{r}$	Average Pore Radius	(L)
$\bar{r}_c$	Capillary Tube Radius	(L)
T	Temperature	(T)
T_R	Reference Temperature $(295°K)$	(T)
u	Diffusion Transport Velocity	(L/t)
V	Volume of Pore	(L^3)
$\bar{v}$	Average Velocity	(L/t)
W	Molar Flow Rate	(moles/t)
y	Mole Fraction	
Z	Compressibility Factor	
α	$1 - |N_B/N_A| = 1 - R_{AB}$	
Δh	Pressure Drop in Inches of Triethylene Glycol Across Capillary Tube	(L)
ϵ	Porosity	
μ	Viscosity	(M/Lt)
π	3.14159	
ρ	Density	(moles/L^3)
σ	Collision Diameter	(L)
Ω_D	Collision Integral for Diffusion	

SUBSCRIPTS

Symbol	Quantity
A	Methane
a	Macropores
B	Propane
c	Capillary Flowmeter
DIFF.	Diffusional Volume
i	Micropores
L	Properties for Face Where $L = L$
0	Properties for Face Where $L = 0$
R	Reference
ωs	Adjusted Overall Porosity for Wakao-Smith and Straight Tube Models

VITA

Howard Sheldon Denenholz

Candidate for the Degree of

Master of Science

Thesis: GASEOUS BINARY COUNTERDIFFUSION IN ACTIVATED CARBON

Major Field: Chemical Engineering

Biographical:

   Personal Data: Born in Chicago, Illinois, July 5, 1943, the son of
      Leonard and Beatrice Denenholz.

   Education: Attended grade school in Chicago, Illinois; graduated
      from Calumet High School, Chicago, in 1961; received the
      Bachelor of Science Degree from the Illinois Institute of
      Technology, Chicago, with a major in Chemical Engineering
      and a minor in Business in June, 1965.

   Professional Experience: Worked as a quality control technician
      and customer service technician for Pyroxylin Products, Inc.,
      Division of Pierce and Stevens Chemical Company during the
      summers of 1962, 1963, 1964, and 1965; member of Omega Chi
      Epsilon Chemical Engineering Honor Society at Oklahoma State
      University; member of Tau Beta Pi Engineering Honor Society
      and Phi Lambda Epsilon Chemistry Honor Society at Illinois
      Institute of Technology; member of American Chemical Society,
      American Institute of Chemical Engineers, and the American
      Association for the Advancement of Science; holder of an
      E.I.T. certificate from the State of Illinois.